

# Quantum random access memory via quantum walk

Ryo Asaka\*, Kazumitsu Sakai† and Ryoko Yahagi ‡

*Department of Physics, Tokyo University of Science,  
Kagurazaka 1-3, Shinjuku-ku, Tokyo, 162-8601, Japan*

August 31, 2020

## Abstract

A novel concept of quantum random access memory (qRAM) employing a quantum walk is provided. Our qRAM relies on a bucket brigade scheme to access the memory cells. Introducing a bucket with chirality *left* and *right* as a quantum walker, and considering its quantum motion on a full binary tree, we can efficiently deliver the bucket to the designated memory cells, and fill the bucket with the desired information in the form of quantum superposition states. Our procedure has several advantages. First, since the bucket is free from any entanglement with the quantum devices at the nodes on the binary tree, our qRAM architecture may be more robust against quantum decoherence. Second, our scheme is fully parallelized. Consequently, only  $O(n)$  steps are required to access and retrieve  $O(2^n)$  data in the form of quantum superposition states. Finally, the simplicity of our procedure may allow the design of qRAM with simpler structures.

## 1 Introduction

The development of an efficient procedure to retrieve classical/quantum data from a database and transform them into a quantum superposition state is one of the most fundamental issues for a practical realization of quantum information processing. Quantum random access memory (qRAM) that stores information and permits queries in superposition may play a pivotal role in a substantial speedup of quantum algorithms for data analysis [1, 2, 3], including applications to machine learning for big data [4, 5, 6, 7, 8].

qRAM is a quantum analogue of classical RAM. Provided a superposition of addresses  $\sum_a |a\rangle$  ( $a \in \mathbb{Z}_{\geq 0}$ ) as input, qRAM accesses the  $a$ th cell in the memory array, where classical information  $|x^{(a)}\rangle$  is stored, and outputs a superposition of  $|x^{(a)}\rangle$ 's correlated with the addresses. Note here that qRAM is possible to store either classical information (i.e. each  $|x^{(a)}\rangle$  does not consist of any superposition of states) or quantum information (i.e. each  $|x^{(a)}\rangle$  is an arbitrary superposition of states). In this letter, we restrict ourselves to the classical case.

---

\*E-mail: 1219502@ed.tus.ac.jp

†E-mail: k.sakai@rs.tus.ac.jp

‡E-mail: yahagi@rs.tus.ac.jp

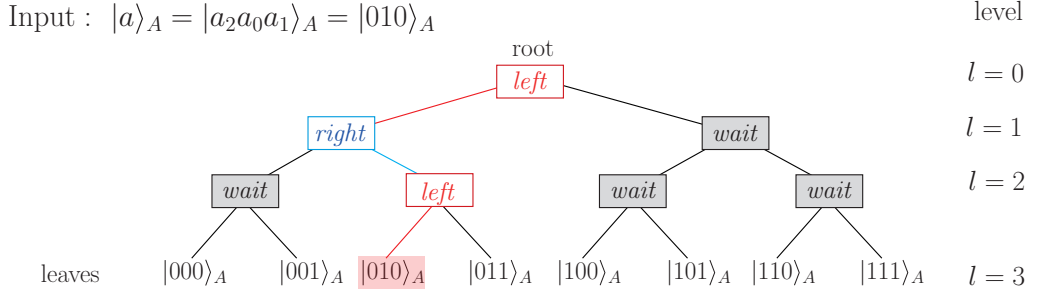


Figure 1: A bucket brigade scheme on the full binary tree with depth  $n = 3$ . The qutrits are equipped at each nodes. To route to the memory cell  $|010\rangle_A$ , one must activate the three qutrits as in the figure.

More precisely, qRAM is defined as

$$\text{qRAM} : \sum_a |a\rangle_A |0\rangle_D \mapsto \sum_a |a\rangle_A |x^{(a)}\rangle_D, \quad (1.1)$$

where  $A$  and  $D$ , respectively, denote quantum analogues of an address register (input register) and a data register (output register). Namely, qRAM (1.1) is a quantum device consisting of (i) a routing scheme to access the designated memory cells, (ii) a querying scheme to retrieving data stored in the cells, and (iii) an output scheme to encode the data into a superposition of quantum states.

As a quantum routing scheme, a notable idea, the ‘‘bucket brigade’’ scheme has been proposed by Giovannetti, Lloyd and Maccone (GLM) [9, 10] to overcome difficulties associated with the conventional fanout scheme commonly implemented in classical RAM (see [11, 12], for instance). The bucket brigade architecture employs a perfect binary tree with  $O(N)$  ( $N = 2^n$ ) ( $n \in \mathbb{Z}_{\geq 0}$ ) nodes routing a signal from the root down to one of the  $N$  leaves interpreted as the memory cells (see Fig. 1 for  $n = 3$ .). Let  $|a_{n-1} \cdots a_0\rangle$  ( $a_l \in \{0, 1\}$ ;  $0 \leq l \leq n-1$ ) be the binary representation of the address of the cell. The value of  $a_l$  indicates the route from a parent node at the  $l$ th level to one of the two children nodes at the  $(l+1)$ th level. For instance, the left (resp. right) child is chosen if  $a_l = 0$  (resp.  $a_l = 1$ ). In consequence, each of the  $N$  possible values of the address register uniquely determines a path in the binary tree.

In the original GLM architecture, a qutrit (i.e. a three-level quantum system with energy levels labeled by *wait*, *left* and *right*) is allocated at each node, and all the qutrits are initialized to be *wait* state. The value  $a_l$  is sequentially delivered from the root to a node at the  $l$ th level, and activates the qutrit to *left* (*right*) if  $a_l = 0$  ( $a_l = 1$ ) to route the following  $a_{l+1}$  to one of the two subsequent nodes. After  $O(n^2)$  time steps, a unique path from the root to the designated memory cell is assigned as depicted in Fig 1 for  $n = 3$  and  $|a\rangle_A = |010\rangle_A$ . Remarkably, only  $n$  qutrits are activated, which is exponentially less than that for the traditional fanout architecture, where  $N$  quantum switches are necessary to be activated. Namely, the GLM bucket brigade architecture has a significant advantage in maintaining quantum coherence.

A quantum signal (the so-called quantum bus) can follow the path to the desired memory cell through the activated qutrits, retrieve information stored in the cell, and goes back to the root along the path. Finally, resetting the activated qutrits to be the initialized state

wait one by one starting from the last level of the tree, one obtains the output as in the r.h.s. of (1.1). That is the GLM bucket brigade qRAM. The GLM scheme has been improved, and concretely implemented into quantum circuits as in [13, 14, 15, 16]. (Note that a different concept of qRAM without relying on any routing scheme has recently been developed in [17].)

This letter provides a novel concept of qRAM, which employs a discrete-time quantum walk as a bucket brigade scheme. A quantum walk is a quantum motion of a particle (interpreted as a bucket) possessing chirality *left* and *right* [18, 19]. The quantum bucket with chirality *left* (resp. *right*) on a parent node moves to the left (resp. right) child node. Each scheme of qRAM can actually be realized by quantum motions of multiple quantum walkers. Our procedure has several advantages. First, the bucket is completely free from any entanglement with the quantum devices at the nodes of the binary tree. Consequently, our qRAM may be much more robust against the decoherence arising from noises at the nodes. Second, each procedure is fully parallelized. As a result, only  $O(n)$  steps are required to access and retrieve data in the form of quantum superposition states. Finally, the three schemes required in qRAM are entirely independent of each other, the architecture of qRAM can be simplified.

The layout of this letter is as follows. In the subsequent section, we introduce a quantum walk on a binary tree. qRAM utilizing the quantum walk is constructed in Sec. 3. In Sec.4, we give some specific examples of how to implement our qRAM scheme using multiple quantum walkers. The last section is devoted to a summary.

## 2 Quantum walk on a binary tree

Quantum walks, which are the quantum counterparts of classical random walks, are defined as a class of unitary time-evolutions on graphs. In contrast to the classical random walks, the randomness comes from a superposition of quantum states and its time evolution. Here, let us introduce a discrete-time quantum walk on a full binary tree. A quantum particle with chirality  $|0\rangle_C$  (*left*) and  $|1\rangle_C$  (*right*) may be interpreted as a quantum “bucket”. A bucket with chirality  $|0\rangle_C$  (resp.  $|1\rangle_C$ ) deviates left (resp. right) at each node of the binary tree, which is contrast to a bucket in the GLM architecture, where the route is determined by activating the qutrit equipped at each node (see the previous section). In consequence, our bucket is free from the entanglement with quantum devices at the nodes, which is one of the main advantages in our scheme.

We consider the full binary tree with depth  $n$  (i.e. it has totally  $2^n$  leaves corresponding to the memory cells) (see Fig. 2 for  $n = 3$ ). Let  $|w, l\rangle_B \in V_{(w,l)} = \mathbb{C}$  denote the position of the  $w$ th node counting from the left in level  $l$  ( $0 \leq w \leq 2^l - 1$ ,  $0 \leq l \leq n$ ), and let us call  $V_B = \bigoplus_{w,l} V_{(w,l)}$  and  $V_C = \mathbb{C}^2$  spanned by the basis  $|0\rangle_C$  and  $|1\rangle_C$  are the “bus space” and “chirality space”, respectively. The quantum walk is defined on the space  $V_B \otimes V_C$ . The quantum walker at the node  $|w, l\rangle_B$  moves to the left (resp. right) child node  $|2w, l+1\rangle_B$  (resp.  $|2w+1, l+1\rangle_B$ ) when the chirality of the walker is  $|0\rangle_C$  (resp.  $|1\rangle_C$ ). This can be represented by the operator  $\mathcal{S}_{(w,l)}$  acting on the space  $(V_{(w,l)} \oplus V_{(2w,l+1)} \oplus V_{(2w+1,l+1)}) \otimes V_C = \mathbb{C}^6$ :

$$\begin{aligned} \mathcal{S}_{(w,l)} : |w, l\rangle_B |0\rangle_C &\mapsto |2w, l+1\rangle_B |0\rangle_C, \\ \mathcal{S}_{(w,l)} : |w, l\rangle_B |1\rangle_C &\mapsto |2w+1, l+1\rangle_B |1\rangle_C. \end{aligned} \quad (2.1)$$

In addition, the walker at the left (resp. right) child node  $|2w, l+1\rangle_B$  (resp.  $|2w+1, l+1\rangle_B$ ) can be pulled back to the parent node  $|w, l\rangle_B$  by  $\mathcal{S}_{(w,l)}$  only if its chirality is  $|0\rangle_C$  (resp.  $|1\rangle_C$ ),

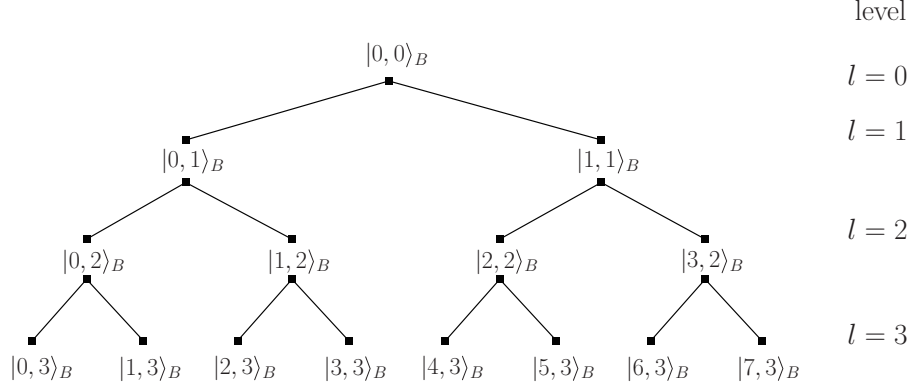


Figure 2: A full binary tree with depth  $n = 3$ . The state  $|w, l\rangle_B$  ( $0 \leq w \leq 2^l - 1$ ,  $0 \leq l \leq n$ ) denotes the position of the  $w$ th node counting from the left in level  $l$ .

and stays at the present position if its chirality is  $|1\rangle_C$  (resp.  $|0\rangle_C$ ). Explicitly,

$$\begin{aligned} \mathcal{S}_{(w,l)} : & |2w, l+1\rangle_B |0\rangle_C \mapsto |w, l\rangle_B |0\rangle_C, \\ \mathcal{S}_{(w,l)} : & |2w+1, l+1\rangle_B |1\rangle_C \mapsto |w, l\rangle_B |1\rangle_C, \\ \mathcal{S}_{(w,l)} : & |2w, l+1\rangle_B |1\rangle_C \mapsto |2w, l+1\rangle_B |1\rangle_C, \\ \mathcal{S}_{(w,l)} : & |2w+1, l+1\rangle_B |0\rangle_C \mapsto |2w+1, l+1\rangle_B |0\rangle_C. \end{aligned} \quad (2.2)$$

Namely,  $\mathcal{S}_{(w,l)}$  is a unitary operator expressed as

$$\begin{aligned} \mathcal{S}_{(w,l)} = & \sum_{i=0}^1 \left( |2w+i, l+1\rangle \langle w, l| + |w, l\rangle \langle 2w+i, l+1| \right)_B \otimes |i\rangle \langle i|_C \\ & + \sum_{i=0}^1 \left| 2w + \frac{1 + (-1)^i}{2}, l+1 \right\rangle \left\langle 2w + \frac{1 + (-1)^i}{2}, l+1 \right|_B \otimes |i\rangle \langle i|_C. \end{aligned} \quad (2.3)$$

Combining a unitary operator  $\mathcal{C}$  acting on  $V_C$ , we obtain a non-trivial quantum motion on the graph. In the next section, we construct  $\mathcal{C}$  such that it acts on both  $V_C$  and the “address space”  $V_A = (\mathbb{C}^2)^{\otimes n}$  to move the quantum walker (bucket) from the root to a specific leaf (memory cell) and to return the bucket filled with information back to the original root.

### 3 qRAM via quantum walk

To appropriately access and retrieve data stored in the specified memory cells in the form of quantum superposition, we employ the quantum walk explained in the previous section. Let

$$\begin{aligned} |x^{(a)}\rangle_D &= |x_{m-1}^{(a)} \cdots x_0^{(a)}\rangle_D = |x_{m-1}^{(a)}\rangle_{D_{m-1}} \cdots |x_0^{(a)}\rangle_{D_0} \quad (x_i^{(a)} \in \{0, 1\}; 0 \leq i \leq m-1), \\ |x_i^{(a)}\rangle \in V_{D_i} &= \mathbb{C}^2, \quad |x^{(a)}\rangle_D \in V_D = \bigotimes_{i=0}^{m-1} V_{D_i} = (\mathbb{C}^2)^{\otimes m} \end{aligned} \quad (3.1)$$

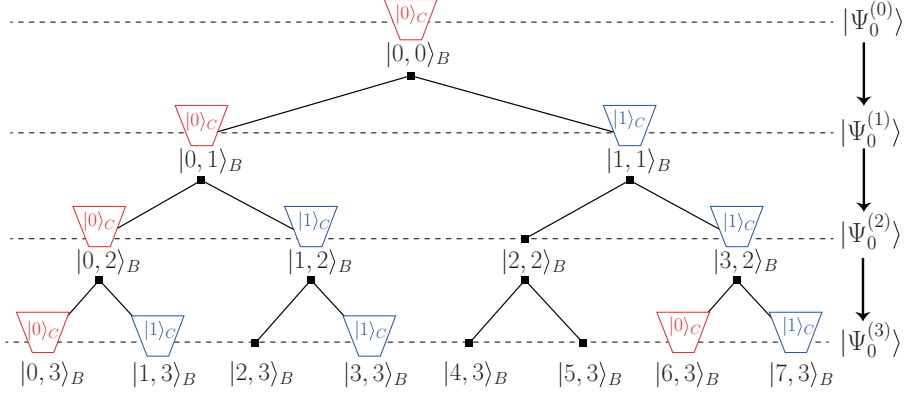


Figure 3: A pictorial representation of the routing scheme (3.7). A bucket with chirality  $|0\rangle_C$  (resp.  $|1\rangle_C$ ) deviates left (resp. right).

be the binary representation of data stored in a memory cell. Here,  $|a\rangle_A$  ( $0 \leq a \leq N - 1$ ;  $N = 2^n$ ) represents the address of the cell:

$$\begin{aligned} |a\rangle_A &= |a_{n-1} \cdots a_0\rangle_A = |a_{n-1}\rangle_{A_{n-1}} \cdots |a_0\rangle_{A_0} \quad (a_i \in \{0, 1\}; 0 \leq i \leq n-1), \\ |a_i\rangle \in V_{A_i} &= \mathbb{C}^2, \quad |a\rangle_A \in V_A = \bigotimes_{i=0}^{n-1} V_{A_i} = (\mathbb{C}^2)^{\otimes n}. \end{aligned} \quad (3.2)$$

Let us call  $V_A$  and  $V_D$  the ‘‘address space’’ and the ‘‘data space’’, respectively. Our qRAM is defined on the space

$$V := V_B \otimes V_C \otimes V_A \otimes V_D \quad (3.3)$$

as

$$\text{qRAM} : \sum_{a \in \mathcal{A}} |0, 0\rangle_B |0\rangle_C |a\rangle_A |0\rangle_D \mapsto \sum_{a \in \mathcal{A}} |0, 0\rangle_B |0\rangle_C |a\rangle_A |x^{(a)}\rangle_D, \quad (3.4)$$

where  $\mathcal{A} \subset \{0, 1, \dots, N - 1\}$ .

As described in Sec. 1, qRAM consists of the following three schemes: (i) a routing scheme to move the empty bucket in a superposition to specific cells, (ii) a querying scheme to fill the bucket with data and (iii) an output scheme to pull back the bucket and output the data in the form of quantum superposition states. Correspondingly, the qRAM is decomposed into the following three operators:

$$\text{qRAM} = \mathcal{F}^\dagger \mathcal{Q} \mathcal{F} \in \text{End}(V). \quad (3.5)$$

(i) *Routing scheme.* First we construct the routing scheme  $\mathcal{F} \in \text{End}(V)$ . Let  $|\Psi_0^{(l)}\rangle \in V$  be a state that the bucket in a superposition is located at nodes in level  $l$  (see Fig. 3 as an example). We set

$$|\Psi_0^{(0)}\rangle = \sum_{a \in \mathcal{A}} |0, 0\rangle_B |0\rangle_C |a\rangle_A |0\rangle_D \quad (3.6)$$

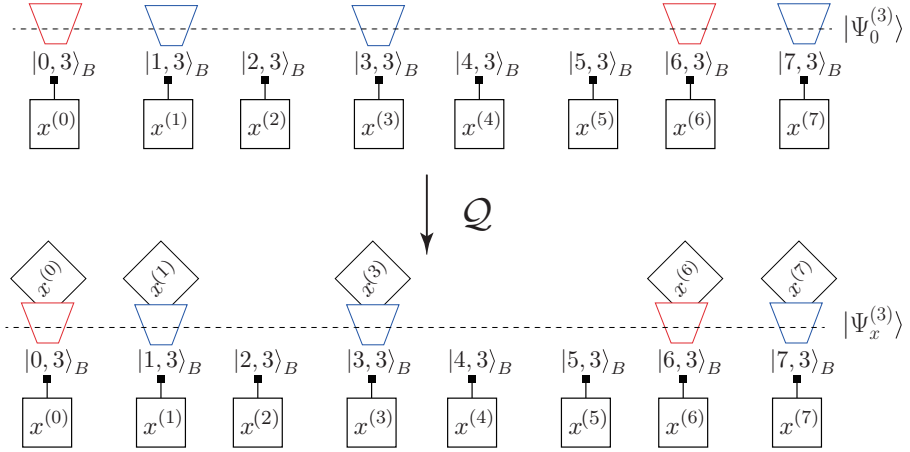


Figure 4: A pictorial representation of the querying scheme (3.12) and (3.13).

as the initial state. One finds that the bucket in a superposition is appropriately delivered to the desired cells at  $\sum_{a \in \mathcal{A}} |a\rangle_A$  by  $\mathcal{F}$ :

$$\mathcal{F} : |\Psi_0^{(0)}\rangle \mapsto |\Psi_0^{(n)}\rangle, \quad (3.7)$$

which is decomposed into  $\mathcal{F} = \mathcal{F}^{(n|n-1)} \dots \mathcal{F}^{(1|0)}$ , where the element  $\mathcal{F}^{(l+1|l)}$

$$\mathcal{F}^{(l+1|l)} : |\Psi_0^{(l)}\rangle \mapsto |\Psi_0^{(l+1)}\rangle, \quad |\Psi_0^{(l)}\rangle := \left| \sum_{k=1}^l 2^{l-k} a_{n-k}, l \right\rangle_B |a_{n-l}\rangle_C |a\rangle_A |0\rangle_D \quad (3.8)$$

is given by

$$\mathcal{F}^{(l+1|l)} := \sum_{w=0}^{2^l-1} \mathcal{S}_{(w,l)} \mathcal{C}_{C,A_{n-(l+1)}} \mathcal{C}_{C,A_{n-l}}. \quad (3.9)$$

Here,  $\mathcal{S}_{(w,l)}$  is the shift operator defined by (2.3) (see also (2.1) and (2.2)) and  $\mathcal{C}_{C,A_l}$  acting non-trivially on  $V_C \otimes V_{A_l}$  is so-called the controlled NOT operator defined as

$$\mathcal{C}_{C,A_l} := I_C \otimes |0\rangle\langle 0|_{A_l} + X_C \otimes |1\rangle\langle 1|_{A_l}, \quad \mathcal{C}_{C,A_n} := I_C, \quad (3.10)$$

where  $X_C, I_C \in \text{End}(V_C)$  are, respectively, the Pauli  $X$  operator and the identity matrix.

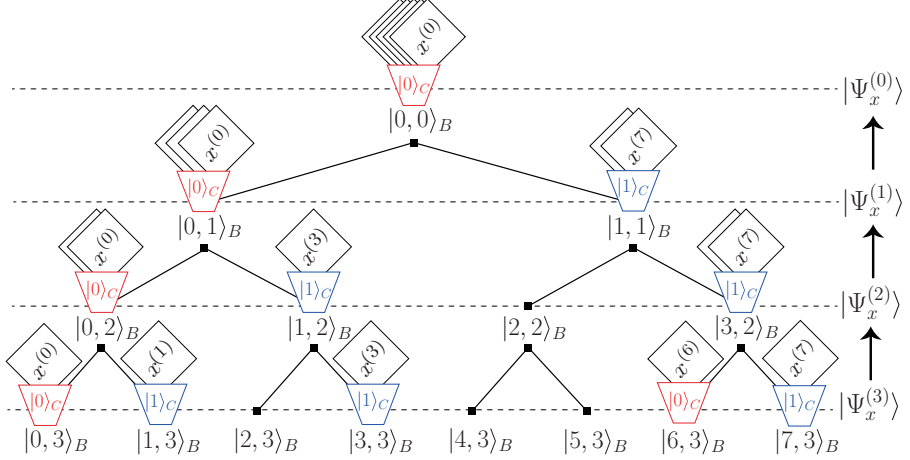


Figure 5: A pictorial representation of the output scheme (3.14).

Eq. (3.8) can be recursively derived as follows:

$$\begin{aligned}
 |\Psi_0^0\rangle &= \sum_{a \in \mathcal{A}} |0,0\rangle_B |0\rangle_C |a\rangle_A |0\rangle_D \xrightarrow{\mathcal{F}^{(1|0)} = \mathcal{S}_{(0,0)} \mathcal{C}_{C,A_{n-1}} \mathcal{C}_{C,A_n}} \\
 |\Psi_0^{(1)}\rangle &= \sum_{a \in \mathcal{A}} |a_{n-1}, 1\rangle_B |a_{n-1}\rangle_C |a\rangle_A |0\rangle_D \xrightarrow{\mathcal{F}^{(2|1)} = (\mathcal{S}_{(0,1)} + \mathcal{S}_{(1,1)}) \mathcal{C}_{C,A_{n-2}} \mathcal{C}_{C,A_{n-1}}} \\
 |\Psi_0^{(2)}\rangle &= \sum_{a \in \mathcal{A}} |2a_{n-1} + a_{n-2}, 2\rangle_B |a_{n-2}\rangle_C |a\rangle_A |0\rangle_D \dots \xrightarrow{\mathcal{F}^{(l|l-1)} = \sum_{w=0}^{2^{l-1}-1} \mathcal{S}_{(w,l-1)} \mathcal{C}_{C,A_{n-l}} \mathcal{C}_{C,A_{n-(l-1)}}} \\
 |\Psi_0^{(l)}\rangle &= \sum_{a \in \mathcal{A}} \left| \sum_{k=1}^l 2^{l-k} a_{n-k}, l \right\rangle_B |a_{n-l}\rangle_C |a\rangle_A |0\rangle_D \dots \xrightarrow{\mathcal{F}^{(n|n-1)} = \sum_{w=0}^{2^{n-1}-1} \mathcal{S}_{(w,n-1)} \mathcal{C}_{C,A_0} \mathcal{C}_{C,A_1}} \\
 |\Psi_0^{(n)}\rangle &= \sum_{a \in \mathcal{A}} |a, n\rangle_B |a_0\rangle_C |a\rangle_A |0\rangle_D. \tag{3.11}
 \end{aligned}$$

Note that, in the last step, we have used  $a = \sum_{k=1}^n 2^{n-k} a_{n-k}$ . As a result, the bucket in a superposition state is delivered to the desired memory cells located at  $\sum_{a \in \mathcal{A}} |a\rangle$ . In Fig. 3, we pictorially show the routing scheme.

One easily sees that  $O(n)$  steps are required for the routing scheme.

(ii) *Querying scheme.* Since our schemes are independent of each other, the querying scheme  $\mathcal{Q} \in \text{End}(V)$  to retrieve information from the memory cells can be significantly simplified and easily parallelized. The operator  $\mathcal{Q}$  defined as

$$\mathcal{Q} : |\Psi_0^{(n)}\rangle \mapsto |\Psi_x^{(n)}\rangle, \quad |\Psi_x^{(n)}\rangle := \sum_{a \in \mathcal{A}} |a, n\rangle_B |a_0\rangle_C |a\rangle_A |x^{(a)}\rangle_D \tag{3.12}$$

can be easily composed by the Pauli  $X$  operator  $X_{D_i} = \text{End}(V_{D_i})$ :

$$\mathcal{Q} := \sum_{a=0}^{2^n-1} |a, n\rangle\langle a, n|_B \otimes \left[ \bigotimes_{i=0}^{2^m-1} (X_{D_i})^{x_i^{(a)}} \right]. \quad (3.13)$$

The querying scheme is shown in Fig. 4. Note that the time steps necessary for the querying scheme is only  $O(1)$ .

(iii) *Output scheme.* Due to the shift operator (2.2), one easily finds that the quantum walk is reversible. Namely, the output scheme to pull back the bucket filled with data can be achieved in exactly the opposite manner as the routing scheme:

$$\mathcal{F}^\dagger : |\Psi_x^{(n)}\rangle \mapsto |\Psi_x^{(0)}\rangle, \quad |\Psi_x^{(0)}\rangle := \sum_{a \in \mathcal{A}} |0, 0\rangle_B |0\rangle_C |a\rangle_A |x^{(a)}\rangle_D. \quad (3.14)$$

See Fig. 5 as an example of the output scheme.

Thus, we find that our qRAM (3.5) satisfies (3.4). The total steps required in our qRAM is  $O(n)$  per memory call.

## 4 Toward a physical implementation

The essential point in our qRAM architecture is the use of a quantum walk: a quantum motion of a particle with chirality. Here, we present some specific examples of how to implement our qRAM architecture using multiple quantum walkers.

One might suspect that our qRAM algorithm (3.4) presented in the previous section could be implemented as a quantum circuit without introducing quantum walks. Of course, it is possible, since (3.4) is defined as a combination of unitary operators. In that case, however, an extra quantum manipulation is required to transfer the value of the address bits, one by one, to a qubit representing the chirality. In this sense, in our algorithm, quantum walks are essential to the efficient implementation of our method. The actual implementation of the qRAM intrinsically using a quantum walk may be achieved by a method proposed in [20], where universal quantum computations via multi-particle quantum walks have been discussed. Quantum gates are defined as scattering processes of quantum walkers.

In total  $n+m$  quantum walkers with chirality  $c$  passing through  $2(n+m)$  different “pipes” represent a state  $|c\rangle_C |a\rangle_A |x^{(a)}\rangle_D$ . For instance, an arbitrary state  $|y\rangle_{A,D} = |y_{n+m-1} \cdots y_0\rangle_{A,D}$

$(y_i \in \{0, 1\}; 0 \leq i \leq n + m - 1)$  with chirality  $|c\rangle_C$  can be represented as

$$\begin{array}{ccc}
 |0\rangle_C | \cdots \underbrace{0}_{y_i} \cdots \rangle = \cdots & \begin{array}{c} |1\rangle \quad |0\rangle \\ \text{---} \quad \text{---} \\ \text{---} \quad \text{---} \\ |y_i\rangle \end{array} & |1\rangle_C | \cdots \underbrace{0}_{y_i} \cdots \rangle = \cdots \\
 & \text{---} & \begin{array}{c} |1\rangle \quad |0\rangle \\ \text{---} \quad \text{---} \\ \text{---} \quad \text{---} \\ |y_i\rangle \end{array} & \text{---} \\
 |0\rangle_C | \cdots \underbrace{1}_{y_i} \cdots \rangle = \cdots & \begin{array}{c} |1\rangle \quad |0\rangle \\ \text{---} \quad \text{---} \\ \text{---} \quad \text{---} \\ |y_i\rangle \end{array} & |1\rangle_C | \cdots \underbrace{1}_{y_i} \cdots \rangle = \cdots \\
 & \text{---} & \begin{array}{c} |1\rangle \quad |0\rangle \\ \text{---} \quad \text{---} \\ \text{---} \quad \text{---} \\ |y_i\rangle \end{array} & \text{---}
 \end{array} \tag{4.1}$$

where the walker with chirality  $|0\rangle_C$  is expressed as the pipe colored red (resp. blue). The superposition states are also characterized by, for instance,

$$\begin{array}{ccc}
 |0\rangle_C | \cdots \underbrace{0}_{y_i} \cdots \rangle + |0\rangle_C | \cdots \underbrace{1}_{y_i} \cdots \rangle = \cdots & \begin{array}{c} |1\rangle \quad |0\rangle \\ \text{---} \quad \text{---} \\ \text{---} \quad \text{---} \\ |y_i\rangle \end{array} & \cdots \\
 & \text{---} & \text{---} \\
 |0\rangle_C | \cdots \underbrace{1}_{y_i} \cdots \rangle + |1\rangle_C | \cdots \underbrace{1}_{y_i} \cdots \rangle = \cdots & \begin{array}{c} |1\rangle \quad |0\rangle \\ \text{---} \quad \text{---} \\ \text{---} \quad \text{---} \\ |y_i\rangle \end{array} & \cdots
 \end{array} \tag{4.2}$$

As a more complicated example, we give

$$|0\rangle_C |0\rangle_A |01^{(0)}\rangle_D + |1\rangle_C |1\rangle_A |10^{(1)}\rangle_D = \begin{array}{c} |1\rangle \quad |0\rangle \\ \text{---} \quad \text{---} \\ \text{---} \quad \text{---} \\ |a_0\rangle_{A_0} \end{array} \quad \begin{array}{c} |1\rangle \quad |0\rangle \\ \text{---} \quad \text{---} \\ \text{---} \quad \text{---} \\ |x_1^{(a)}\rangle_{D_1} \end{array} \quad \begin{array}{c} |1\rangle \quad |0\rangle \\ \text{---} \quad \text{---} \\ \text{---} \quad \text{---} \\ |x_0^{(a)}\rangle_{D_0} \end{array}, \tag{4.3}$$

where (0) and (resp. (1)) in the r.h.s. denotes the correlation with the particle representing the address  $a_0 = 0$  (resp.  $a_0 = 1$ ). Thus the state  $\Psi_0^{(l)}$  or  $\Psi_x^{(l)}$  can be expressed by  $n + m$

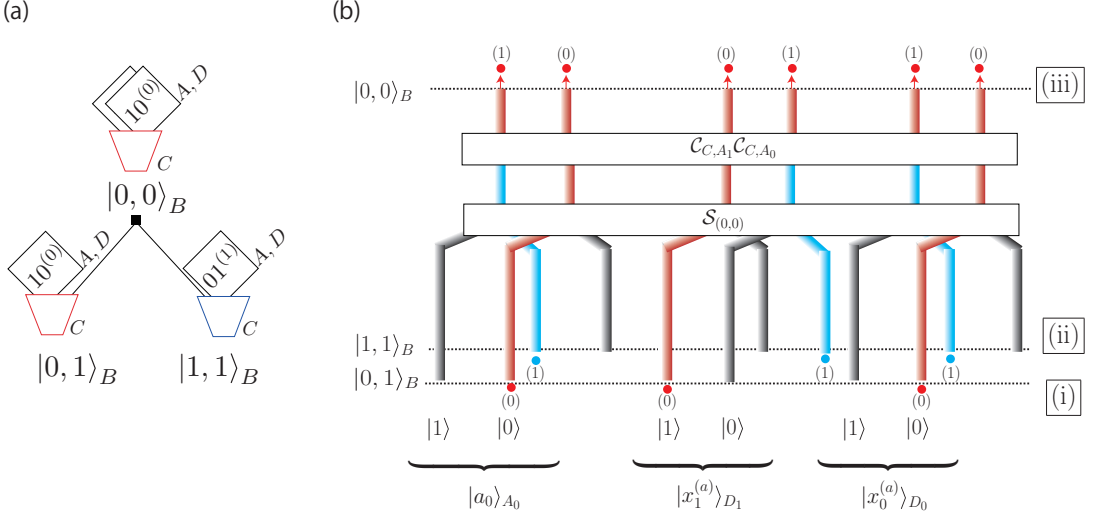


Figure 6: (a): An example of the output scheme  $\mathcal{F}^\dagger$  (4.4) at a node  $|0,0\rangle_B$  for  $n = 1$  and  $m = 2$ . (b): A representation of (a) by quantum walkers (see also (4.1)–(4.3) as examples of the representation of states). (i), (ii) and (iii) represents the states (i)  $|0,1\rangle_B|0\rangle_C|0\rangle_A|10^{(0)}\rangle_D$ , (ii)  $|1,1\rangle_B|1\rangle_C|1\rangle_A|01^{(1)}\rangle_D$  and (iii)  $|0,0\rangle_B|0\rangle_C(|0\rangle_A|10^{(0)}\rangle_D + |1\rangle_A|01^{(1)}\rangle_D)$ , respectively.

quantum walkers and their superpositions passing through the different  $2(n+m) \times 2^l$  pipes. In Fig 6, we depict an example of the output scheme (3.14) for  $n = 1$  and  $m = 2$ .

$$\begin{aligned} \mathcal{F}^\dagger : & |0,1\rangle_B|0\rangle_C|0\rangle_A|10^{(0)}\rangle_D + |1,1\rangle_B|1\rangle_C|1\rangle_A|01^{(1)}\rangle_D \\ & \mapsto |0,0\rangle_B|0\rangle_C \left( |0\rangle_A|10^{(0)}\rangle_D + |1\rangle_A|01^{(1)}\rangle_D \right). \end{aligned} \quad (4.4)$$

## 5 Concluding remarks

In summary, we have provided a new concept of bucket brigade qRAM utilizing a quantum walk. Controlling a quantum motion of the quantum bucket with chirality, we can efficiently deliver the bucket to the desired memory cell, and fill the bucket with data stored in cells. Since our qRAM does not rely on quantum switches for the routing scheme, the bucket is free from the entanglement with the nodes. Therefore, our qRAM may be more robust against quantum decoherence. Furthermore, the simplicity of our scheme makes it possible to design qRAM with simpler structures.

Quantum walks have been actually implemented as quantum circuits [20, 21, 22]. An implementation of our qRAM algorithm as a quantum circuit remains a future issue. It may also be of interest to apply our qRAM to quantum information processing, for instance image processing and transformations utilizing quantum version of fast Fourier transform [23], where the generation of multiple quantum images is crucial.

## Acknowledgment

The present work was partially supported by Grant-in-Aid for Scientific Research (C) No. 20K03793 from the Japan Society for the Promotion of Science.

## References

- [1] Grover L K 1996 A fast quantum mechanical algorithm for database search *Proc. ACM STOC* 212-219
- [2] Harrow A W, Hassidim A and Lloyd S (2009) Quantum algorithm for linear systems of equations *Phys. Rev. Lett.* **103** 150502
- [3] Lloyd, S, Mohseni M, Rebentrost P 2014 Quantum principal component analysis *Nature Physics* **10** 631
- [4] Lloyd S, Mohseni M, Rebentrost P 2013 Quantum algorithms for supervised and unsupervised machine learning *arXiv:1307.0411*
- [5] Rebentrost P, Mohseni M and Lloyd S 2014 Quantum support vector machine for big data classification *Phys. Rev. Lett.* **113** 130503
- [6] Biamonte J, Wittek P, Pancotti N, Rebentrost P, Wiebe N and Seth Lloyd S 2017 Quantum machine learning *Nature* **549** 195-202
- [7] Schuld M, Fingerhuth M, Petruccione F 2017 Implementing a distance-based classifier with a quantum interference circuit *Europhys. Lett.* **119** 60002
- [8] Bang J, Dutta A, Lee S W, and Kim J 2019 Optimal usage of quantum random access memory in quantum machine learning *Phys. Rev. A* **99** 012326
- [9] Giovannetti V, Lloyd S and Maccone L 2008 Quantum Random Access Memory *Phys. Rev. Lett.* **100** 160501
- [10] Giovannetti V, Lloyd S and Maccone L 2008 Architectures for a quantum random access memory *Phys. Rev. A* **78** 052310
- [11] Jaeger R C and Blalock T N 2003 *Microelectronic Circuit Design* (Dubuque, IA: McGraw-Hill)
- [12] Sedra A S and Smith K C 1998 *Microelectronic Circuits* (New York: Oxford University Press)
- [13] Hong F-Y, Xiang Y, Zhu Z-Y, Jiang L-z and Wu L-n 2012 Robust quantum random access memory *Phys. Rev. A* **86** 010306
- [14] Arunachalam S, Gheorghiu V, Jochym-OfConnor T, Mosca M and P. V. Srinivasan P V 2015 On the robustness of bucket brigade quantum RAM *New J. Phys.* **17** 123010

- [15] Matteo O D, Gheorghiu V and Mosca M 2020 Fault-Tolerant Resource Estimation of Quantum Random-Access Memories *IEEE Transactions on Quantum Engineering* **1** 4500213
- [16] Paler A, Oumarou O and Basmadjian R 2020 Parallelising the Queries in Bucket Brigade Quantum RAM *arXiv*: 2002.09340
- [17] Park D K, Petruccione F and Rhee J-K K 2019 Circuit-Based Quantum Random Access Memory for Classical Data *Sci. Rep.* **9**:3949
- [18] Aharonov Y, Davidovich L, Zagury N 1993 Quantum random walks *Phys. Rev. A* **48** 1687
- [19] Venegas-Andraca, S E 2012 Quantum walks: a comprehensive review *Quantum Inf. Process.* **11** 1015
- [20] Andrew M. Childs A M, Gosset D and Webb Z 2013 Universal Computation by Multi-particle Quantum Walk *Science* **339** 791
- [21] Childs A M 2009 Universal Computation by Quantum Walk *Phys. Rev. Lett.* **102** 180501
- [22] Lovett N B, Cooper S, Everitt M, Trevers M and Kendon V 2010 Universal quantum computation using the discrete-time quantum walk *Phys. Rev. A* **81** 042330
- [23] Asaka R, Sakai K, and Yahagi R 2020 Quantum circuit for the fast Fourier transform *Quantum Inf. Process.* **19** 277